

UC Santa Cruz

UC Santa Cruz Previously Published Works

Title

Algal Kainoid Synthases Exhibit Substrate-Dependent Hydroxylation and Cyclization Activities.

Permalink

<https://escholarship.org/uc/item/07w4d33p>

Journal

ACS Chemical Biology, 18(12)

Authors

Hopiavuori, Austin

McKinnie, Shaun

Publication Date

2023-12-15

DOI

10.1021/acscchembio.3c00596

Copyright Information

This work is made available under the terms of a Creative Commons Attribution-NonCommercial-NoDerivatives License, available at

<https://creativecommons.org/licenses/by-nc-nd/4.0/>

Peer reviewed

Algal Kainoid Synthases Exhibit Substrate-Dependent Hydroxylation and Cyclization Activities

Austin R. Hopiavuori and Shaun M. K. McKinnie*

Cite This: *ACS Chem. Biol.* 2023, 18, 2457–2463

Read Online

ACCESS |



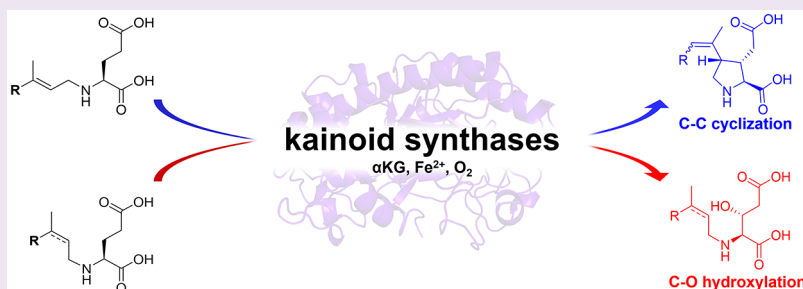
Metrics & More



Article Recommendations



Supporting Information



ABSTRACT: Fe^{II}/ α -ketoglutarate-dependent dioxygenases (Fe/ α KG) make up a large enzyme family that functionalize C–H bonds on diverse organic substrates. Although Fe/ α KG homologues catalyze an array of chemically useful reactions, hydroxylation typically predominates. Microalgal DabC uniquely forms a novel C–C bond to construct the bioactive pyrrolidine ring in domoic acid biosynthesis; however, we have identified that this kainoid synthase exclusively performs a stereospecific hydroxylation reaction on its *cis* substrate regioisomer. Mechanistic and kinetic analyses with native and alternative substrates identified a 20-fold rate increase in DabC radical cyclization over β -hydroxylation with no observable 1,5-hydrogen atom transfer. Moreover, this dual activity was conserved among macroalgal RadC1 and KabC homologues and provided insight into substrate recognition and reactivity trends. Investigation of this substrate-dependent chemistry improves our understanding of kainoid synthases and their biocatalytic application.

The nonheme iron/ α -ketoglutarate-dependent dioxygenases (Fe/ α KGs) are a large and diverse enzyme family widely distributed throughout nature in both primary and secondary metabolism.^{1,2} Fe/ α KGs catalyze a variety of valuable transformations at unactivated C–H bonds, including halogenations, desaturations, epoxidations, ring formations, expansions, and contractions; however, hydroxylation reactions are the most prevalent.^{1,2} Structurally, Fe/ α KGs have a conserved double-stranded β -helix (DSBH) fold with a Fe(II)-binding facial triad. In the presence of atmospheric oxygen and α KG cosubstrate, these enzymes generate a high-energy Fe(IV)-oxo species capable of radically abstracting a hydrogen atom from the targeted carbon center of the substrate.^{1,2} Outside their important regulatory roles on macromolecular substrates and in primary metabolism,¹ Fe/ α KG hydroxylases are involved in the biosynthesis of natural products in diverse biological species. A number of dioxygenases act on amino acid substrates, which can be further functionalized and/or incorporated into complex natural product syntheses (Figures 1A, S1).³ Notable examples include bacterial VioC and TauD and fungal IboH, which stereospecifically hydroxylate L-arginine, taurine, and L-glutamic acid, respectively (Figure 1A, S1).^{4–6} One rare reaction that this family catalyzes is C–C bond formation; of

the hundreds of characterized Fe/ α KG enzymes, only a few have been confirmed to function as C–C bond forming cyclases (Figures 1A, S1).⁷ Cyclization reactions are significant in natural product biosynthesis to rigidify molecules into favorable binding positions, thereby improving target specificity and potency. Recent examples of Fe/ α KGs from diverse organisms that perform C–C bond cyclization reactions include: BelL and HrmJ from belactosin A and hormaomycin biosyntheses in *Streptomyces* bacteria that catalyze the diastereodivergent *trans*-nitrocyclopropanation of 6-nitro-L-norleucine⁸ and 2-ODD from the plant podophyllotoxin biosynthetic pathway that assembles the core tetracyclic scaffold from (–)-yatein en route to the valuable chemotherapeutic etoposide (Figures 1A, S1).^{9,10} Notably, algal kainoid synthase DabC from the diatom *Pseudo-nitzschia multiseries* and homologues RadC1 and KabC from red macroalgae *Chondria armata* and *Digenea simplex* cyclize *N*-

Received: September 26, 2023

Revised: November 28, 2023

Accepted: November 29, 2023

Published: December 4, 2023



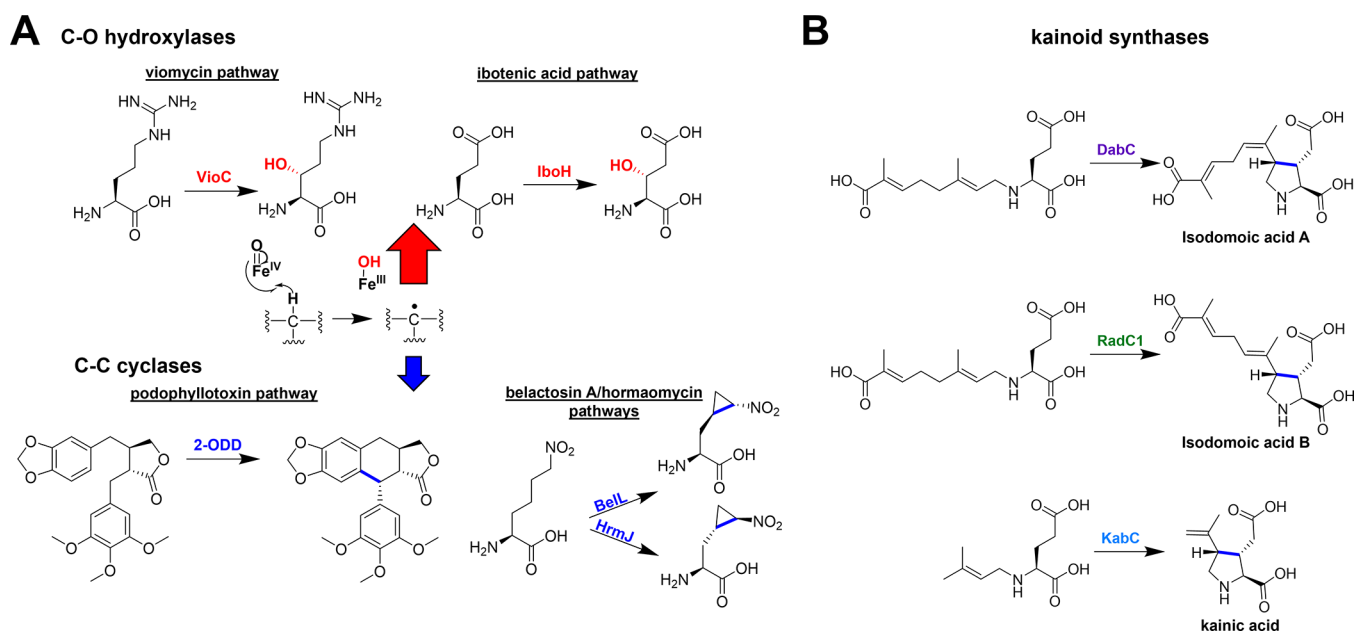


Figure 1. (A) Select examples of Fe/ α KG-catalyzed hydroxylation (top, red) and C–C cyclization (bottom, blue) reactions from various natural product biosynthetic pathways. (B) Reactions of micro- and macroalgal kainoid synthases DabC, RadC1, and KabC.

prenylated L-glutamic acids to construct the pyrrolidine moieties of domoic acid (DA) and kainic acid (KA) (Figure 1B).^{11–13}

DA is a potent neurotoxic natural product that agonistically binds ionotropic glutamate receptors (iGluRs) in the central nervous system, thereby causing neuronal excitotoxicity through enhanced Ca^{2+} accumulation.¹⁴ The release of DA during marine harmful algal blooms has had an increasingly devastating environmental impact on wildlife, and human exposure via consuming contaminated seafood causes amnesic shellfish poisoning.¹⁵ Seaweed-derived KA has a reduced agonistic effect compared with DA and is employed experimentally to investigate epilepsy and other neurological disorders.¹² The key structural feature imparting improved iGluR agonism is the pyrrolidine moiety formed following the action of DabC and homologues. This kainoid ring stabilizes the glutamic acid side chain in an advantageous binding orientation, which rationalizes its improved potency relative to its endogenous L-Glu ligand.¹⁴ It is not clear how kainoid synthases divert Fe/ α KG hydroxylation to preferentially catalyze this bioactive C–C bond-forming cyclization, which leads to the basis of our current investigation. Mechanistic and structural insights into DabC and homologues not only improve our basic science understanding of Fe/ α KG enzymology but concurrently enable their downstream biocatalytic application toward diverse and putatively neuroactive kainoid scaffolds.

We initially aimed to investigate the range of non-native substrates DabC can recognize and transform and adapted established protocols for heterologous DabC expression in *Escherichia coli* and purification via Ni-NTA affinity chromatography. Validated DabC substrate *trans*-7'-carboxygeranyl-N-L-glutamic acid (**1-trans**) was synthesized alongside its minor *cis*-regioisomer byproduct (*cis*-7'-carboxyneryl-N-L-glutamic acid; **1-cis**) following reductive amination of L-glutamic acid with 7-carboxygeranial.¹¹ Similar to previous reports, DabC efficiently converted **1-trans** to major product isodomoic acid A (**2**) in the presence of necessary cofactors and cosubstrates

(Fe^{2+} , α KG, L-ascorbate, and O_2) following *in vitro* assays and ultrahigh-performance liquid chromatography–mass spectrometry (UPLC-MS) analyses.¹¹ However, when employing regioisomer **1-cis** under identical reaction conditions, negligible cyclic and/or dehydrogenated product [M-2H] extracted ion chromatograms (EICs) were detected. Instead, the new putatively hydroxylated [M+O] product **3** was exclusively observed (Figure 2A). When a purified mixture of both substrate isomers (**1-mix**) was used for *in vitro* DabC assays, both cyclic **2** and hydroxylated **3** products were observed in ratios comparable with those of the individually purified regioisomers, thus simplifying our downstream workflow to isolate and characterize **3**. A DabC reaction with **1-mix** was performed on a 25 mg scale, isolating **3** after reversed-phase high-performance liquid chromatography (RP-HPLC). Following 1D and 2D nuclear magnetic resonance (NMR) spectroscopy and high-resolution mass spectrometry (HRMS), **3** was confirmed to be hydroxylated at the β -position of glutamic acid while maintaining the *cis*-configuration at the allyl amine. Intriguingly, *N*-geranyl-(3*R*)-hydroxy-L-glutamic acid was isolated in microgram quantities from domoic acid-producing *C. armata*.¹⁶ Comparison of the glutamate moiety ^1H and ^{13}C NMR chemical shifts between **3** and this red algal metabolite supported that the β -hydroxy group was installed at the pro-*R* hydrogen (Tables S1 and S2).¹⁶ To unequivocally assign the stereochemistry of **3**, 3*R*-hydroxy-L-glutamic acid was enantioselectively synthesized from L-malic acid^{17,18} and then condensed with 7-carboxygeranial via reductive amination. Regioisomers were separated by RP-HPLC, and enzymatic **3** proved to be identical to synthetic 7'-carboxy-*N*-neryl-(3*R*)-hydroxy-L-glutamic acid by UPLC-MS retention time (Figure 2A) and NMR (Figure 2B; Tables S1 and S2). This validates that Fe/ α KG homologue DabC is capable of both hydroxylation and cyclization biochemistries with relatively conservative substrate alterations.

To rationalize these divergent enzymatic functions and products, we propose that DabC initially abstracts the pro-*R* glutamic acid β -hydrogen on both substrates (Figure 2C).

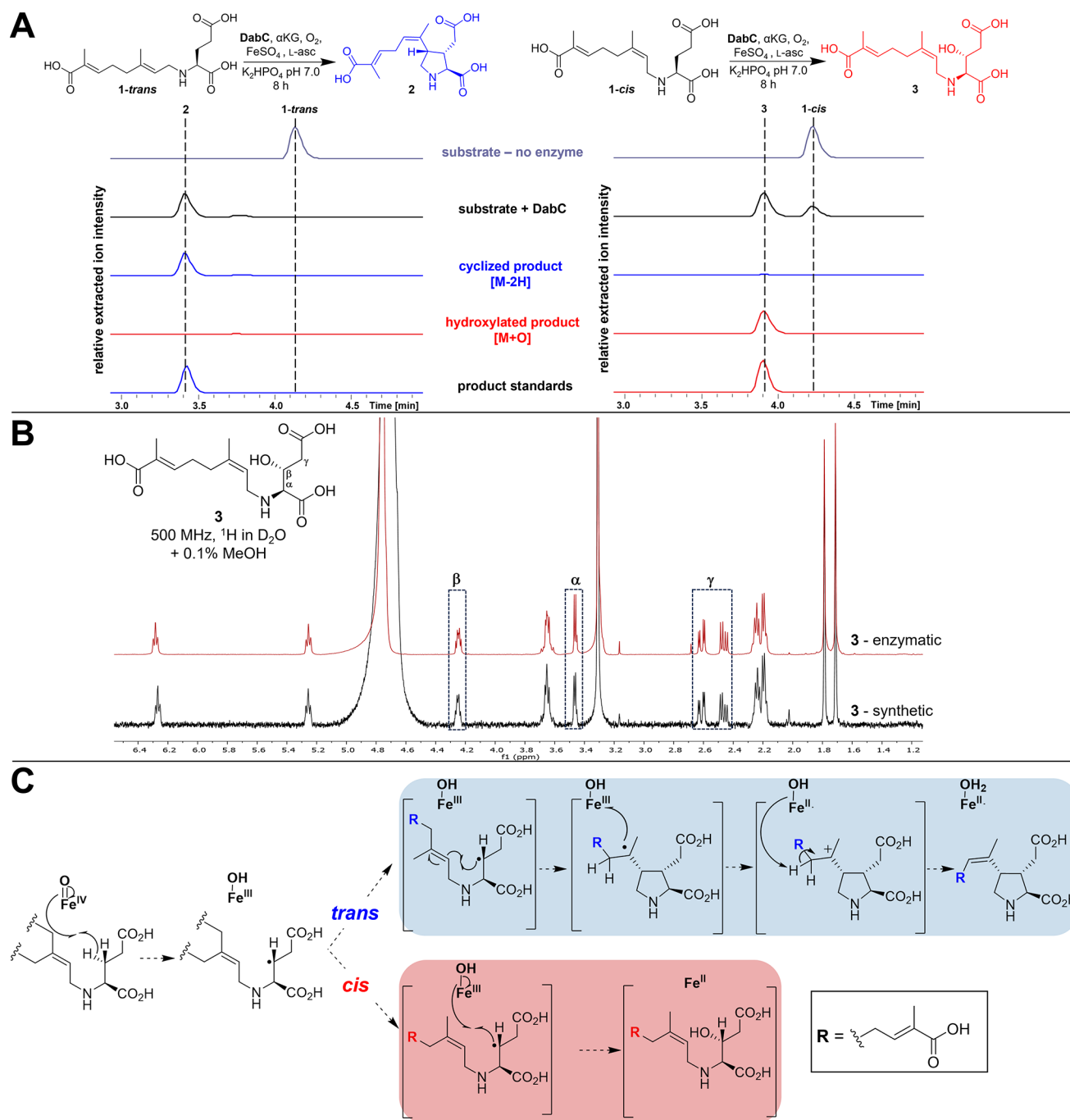


Figure 2. DabC preferentially hydroxylates the *cis* regioisomer of its native substrate. (A) Analytical DabC assays with either **1-trans** (left) or **1-cis** (right) as the substrate. Relative intensities of negative mode extracted ion chromatograms (EICs) from UPLC-MS traces in the absence (gray trace) and presence (black trace) of DabC. Assays were extracted for substrate **1**, cyclic product **2** (blue trace), and hydroxylated product **3** (red trace) ($[M-H]^-$ 312.15, 310.12, 328.14 ± 0.3 *m/z*, respectively) and compared with purified **2** and synthetic **3** standards. (B) ¹H NMR overlay of synthetic **3** (black) and enzymatic product **3** (red) with labeled glutamate side-chain signals. (C) Mechanistic proposal for divergent DabC activities with *cis* (red) and *trans* (blue) substrates.

However, the mechanism then deviates depending on allyl amine stereochemistry. Non-native **1-cis** undergoes a canonical Fe/αKG hydroxyl rebound from the iron cofactor to generate stereoselectively β-hydroxylated **3**. In contrast, **1-trans** completes a radical 5-*exo-trig* cyclization to construct a novel carbon–carbon bond and sets the last of the three contiguous stereocenters of the kainoid ring. Electron transfer to the Fe(III)–OH intermediate followed by regioselective deprotonation adjacent to the tertiary carbocation completes the

“interrupted desaturase” mechanism in the production of **2** (Figure 2C).^{11,19} To experimentally corroborate this mechanism and confirm that only one hydrogen atom is being abstracted from glutamate in both reactions, a glutamate-backbone *d*₅-labeled mixture of native substrate isomers (*d*₅-**1-mix**) was prepared. The overnight incubation of *d*₅-**1-mix** with DabC indicated the loss of one deuterium within both cyclic (*d*₄-**2**) and hydroxylated (*d*₄-**3**) products by UPLC-MS (Figure S2), which supports a radical mechanism for both

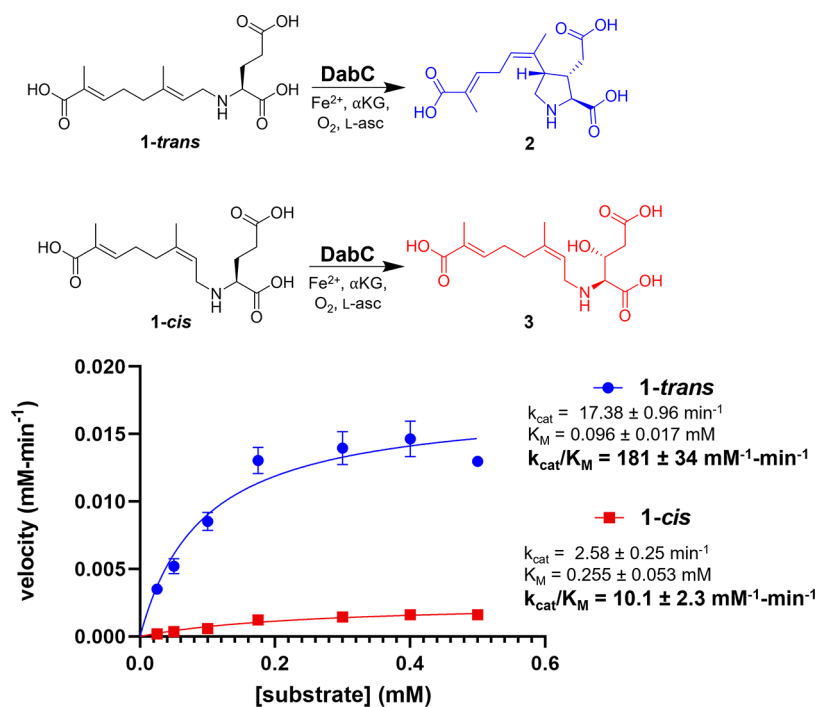


Figure 3. Michaelis–Menten kinetic parameters for the DabC-catalyzed cyclization reaction of 1-*trans* (blue) compared with the β -hydroxylation reaction with 1-*cis* (red).

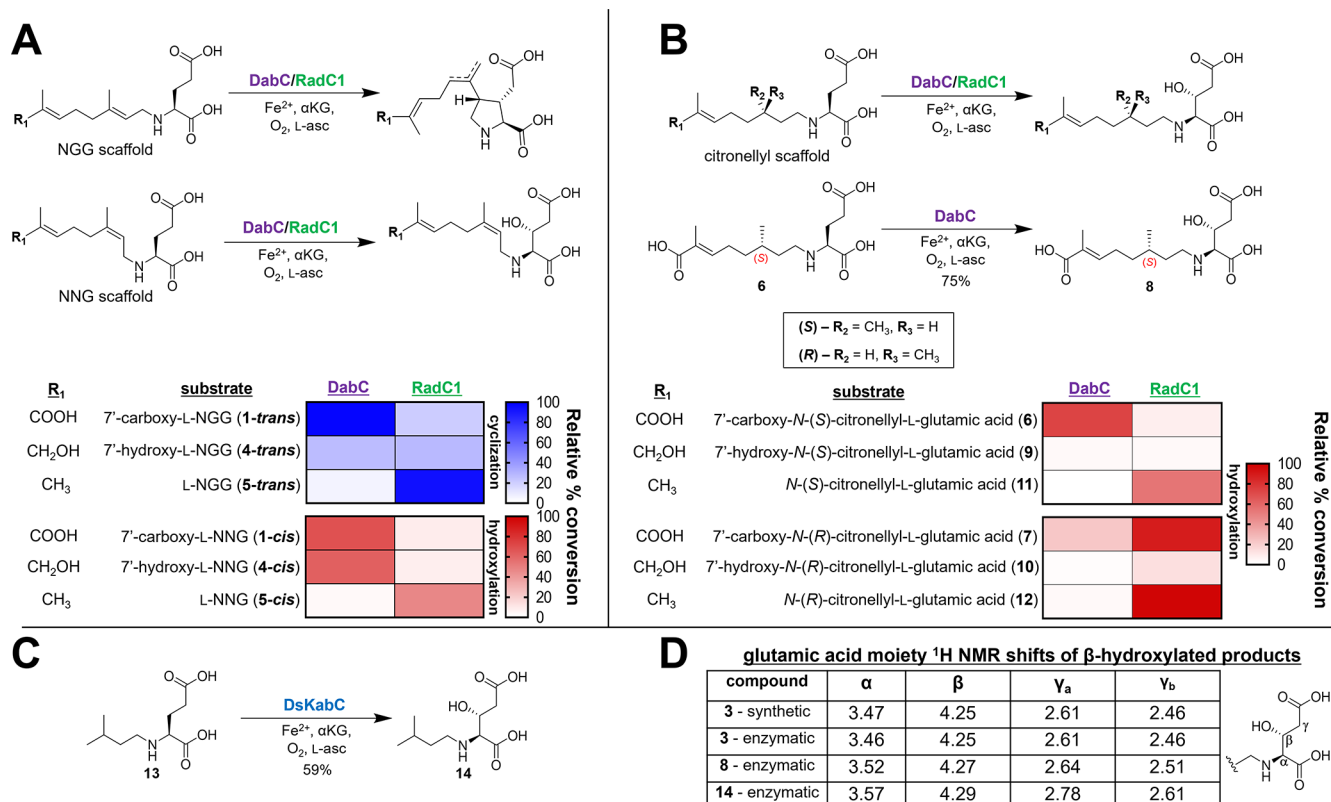


Figure 4. Hydroxylation activity on alternative substrates is conserved across kainoid synthase homologues DabC, RadC1, and KabC. (A) General reaction schemes for *in vitro* reactions of NGG and NNG substrate analogues with 7'-modifications (1, 4, 5) by DabC and RadC1. Heat maps indicating the relative % conversion to cyclic (blue) or β -hydroxylated products (red). (B) General reaction scheme for *in vitro* reactions of citronellyl substrate analogues by DabC and RadC1 with scaled-up DabC production of 8 shown underneath. Heat maps indicating the relative % conversion of *N*-citronellyl analogues to β -hydroxylated products. (C) *In vitro* β -hydroxylation of *N*-isopentyl-L-glutamic acid (13) by DsKabC. (D) Comparison of ^1H NMR shifts for the glutamic acid moiety in isolated β -hydroxylated products.

products. To assess DabC stereospecificity, the substrate enantiomer mixture was synthesized (**D-1-mix**) and incubated with DabC. No definitive cyclic, desaturated, or hydroxylated products could be detected by UPLC-MS, which suggests that DabC possesses a high degree of stereospecificity for both enzymatic functions (Figure S3). To probe the catalytic differences between the DabC cyclization and hydroxylation reactions, *in vitro* kinetics assays were conducted with **1-trans** and **1-cis**. Conditions were initially optimized with **1-mix** to improve the overall conversion efficiency of DabC for both products in comparison with a chloramphenicol (CAM) internal standard. Buffer pH (Figure S4), cofactor (Figures S5 and S6), and cosubstrate concentrations (Figure S7) were independently assessed over a range of values using 5 mol % DabC and 14 h reaction conditions. Individual end points that displayed the highest relative conversion for compounds **2** and **3** were selected for *in vitro* kinetic assays. Optimized assay conditions [pH 6.0, 1.0 mM iron(II) sulfate, 50 mM α -ketoglutarate, and 0.1 mM L-ascorbate] were compared with the literature, and the hydroxylation reaction showed the most notable conversion improvement (Figure S8). After preparing standard curves for major products **2** and **3** (Figure S9), DabC steady-state kinetics experiments were individually performed with **1-trans** and **1-cis** substrates under a range of enzyme/substrate ratios while all other cosubstrate and cofactor concentrations were held constant. Michaelis–Menten kinetic parameters were determined for both substrate regioisomers to reveal that DabC has a nearly 20-fold greater apparent k_{cat}/K_M for the cyclization of **1-trans** relative to the hydroxylation of **1-cis** (Figure 3). The binding affinity for **1-trans** was surprisingly not substantially different than **1-cis** (0.096 and 0.255 mM, respectively); instead, the first-order rate constant (k_{cat}) was the most significant contributor to the difference in catalytic efficiency between substrates. The 7-fold increase in turnover rate for **2** versus **3** production (17.4 and 2.6 min⁻¹) was intriguing given the mechanistic complexity of **1-trans** carbon–carbon bond formation, electron transfer, and desaturation compared with the **1-cis** hydroxyl rebound. To further investigate the substrate effects on enzyme activity and α -ketoglutarate cosubstrate consumption, succinate/product formation ratios were determined for both **1-trans** and **1-cis** after *in vitro* DabC assays. The hydroxylation reaction with **1-cis** was found to have a ratio of succinate/**3** formation (1.26 \pm 0.37), which was not significantly different than the cyclization reaction on **1-trans** (0.94 \pm 0.28 succinate/**2** formation). This suggests that DabC can perform divergent chemical reactions with a comparable level of substrate and cosubstrate consumption (Figure S10). To provide preliminary structural insight into these divergent enzymatic activities, **1-trans** and **1-cis** were individually docked into an AlphaFold model of DabC. The superimposed lowest-energy conformations suggest differential positioning of the glutamic acid side chain between both substrates, with the target β -carbon of **1-cis** in closer proximity to the coordinated iron cofactor (Figure S11). These *in silico* observations could help rationalize the mechanistic differences between these two reactions; however, additional biochemical and structural interrogation would be required.

We next wanted to assess how substrate analogues affect the extent of DabC conversion for both cyclization and hydroxylation. Previous efforts identified a pronounced reduction in kainoid product formation when interrogating DabC with *N*-geranylated L-glutamic acids lacking the 7'-carboxylic acid moiety.^{11,20} We wanted to see if modifications

at the distal end would have a comparable impact on β -hydroxylation activity. Literature protocols were adapted to synthesize 7'-hydroxy (**4**)- and 7'-methyl (**5**)-modified *trans* (*N*-geranyl L-glutamic acid; L-NGG) and *cis* (*N*-neryl L-glutamic acid; L-NNG) substrates (Figure 4A).¹¹ *In vitro* DabC assays followed by UPLC-MS analyses confirmed that **4-cis** and **5-cis** analogues were preferentially hydroxylated (Figures S12 and S13). The extent of conversion was relatively assessed by comparing the intensity of the EIC for the major enzymatic product to that of the original substrate, thereby assuming similar ionization efficiencies for both molecules. These assays corroborated the 7'-substitution recognition trends where a decrease in both cyclization and hydroxylation activities followed decreasing 7'-position oxidation (Figures 4A, S12). The recent characterization of red macroalgal homologue RadC1 (63% DabC sequence identity),¹³ which preferentially cyclizes **1-trans** to isodomoic acid **B** (Figure 1B), provided an opportunity to assess whether kainoid synthases from biologically diverse organisms exhibit similar 7'-position reactivity trends. After the heterologous expression, purification, and *in vitro* interrogation with our focused 7'-modified L-NGG and L-NNG substrate panel, *C. armata* RadC1 also exhibited substrate-dependent biochemistries. All examined *trans* isomers (**1-trans**, **4-trans**, and **5-trans**) were converted by RadC1 into putative cyclic and/or dehydrogenated [M–2] products, while *cis* isomers (**1-cis**, **4-cis**, and **5-cis**) were hydroxylated following UPLC-MS analyses (Figures 4A, S14). Two major differences were observed: RadC1 preferred both 7'-methyl-substrates (**5-trans**, **5-cis**) under our optimized *in vitro* conditions, and **4-cis** was effectively hydroxylated by DabC (62 \pm 2%) but less tolerated by RadC1 (8 \pm 2%) (Figures 4A, S12, and S14). While the structural basis of 7'-recognition is still under investigation, we were encouraged to see that similar reactivity patterns emerged for both homologues.

The *5-exo-trig* cyclization mechanism catalyzed by DabC and its homologues involves the radical interception of the substrate 2'-allyl amine.^{11,19} We hypothesized that the removal of this alkene would divert kainoid synthases to exclusively hydroxylate substrates. Given the utility of intramolecular 1,5-hydrogen atom transfer (1,5-HAT) in chemosynthetic²¹ and Fe/ α KG biocatalytic reactions²² and the propensity of DabC to cyclize **1-trans**, it was unclear if regioselective β -hydroxylation or 1,5-HAT followed by distal hydroxylation would predominate with saturated analogues (Figure S15). We used both commercially available citronellol enantiomers to divergently synthesize two novel 7'-carboxy-*N*-citronellyl-L-glutamic acid substrates with *S* (**6**) or *R* (**7**) 3'-methyl stereochemistries. *In vitro* interrogation of DabC and RadC1 with **6** and **7** exclusively showed a new hydroxylated product in the presence of all cofactors and cosubstrates (Figures 4B, S16, and S17). To validate the regioselectivity of product hydroxylation, the DabC assay with **6** was scaled up, purified via RP-HPLC, and characterized as 7'-carboxy-*N*-(3'*S*)-citronellyl-3*R*-hydroxy-L-glutamic acid (**8**) following NMR and HRMS (Figure 4B). The two tested homologues had an intriguing conversion preference: DabC preferentially hydroxylated *S*-isomer **6**, whereas **7** was much better tolerated by RadC1 under the conditions employed. Given the improved *in vitro* conversion of RadC1 with **5-trans** and **5-cis**, we used *S*- or *R*-citronellal enantiomers to divergently synthesize four additional saturated analogues with 7'-hydroxy or 7'-methyl end permutations (**9**–**12**). UPLC-MS analyses of *in vitro*

assays revealed that *N*-citronellyl substrate analogues were hydroxylated by both kainoid synthases, which mirrored both the 7'-substitution and 3'-methyl stereochemical trends observed with 1/4/5 and 6/7 substrate analogues, respectively (Figures 4B, S16, and S17). Comparison of DabC and RadC1 AlphaFold models with docked 1-*trans* identified highly conserved amino acid residues in putatively structured regions surrounding the 3'-methyl and 7'-positions. Variability in isodomoic acid regioisomer production is presumably due to pocket shape and/or second shell differences, as previously proposed (Figure S18).¹³ To extend our investigation to *D. simplex* KabC, (DsKabC; 60% DabC sequence identity), saturated analogue *N*-isopentyl-L-glutamic acid (13) was synthesized and incubated with the KA-producing Fe/ α KG homologue.¹² UPLC-MS analysis confirmed the presence of a hydroxylated product, which was identified as *N*-isopentyl-(3*R*)-hydroxy-L-glutamic acid (14) following NMR and HRMS characterization (Figures 4C, S19). Hydroxylated product EICs were previously observed following DsKabC incubation with *N*-isopentyl and *N*-benzyl L-glutamic acid substrates; however, neither were structurally validated.¹⁹ Comparison of enzymatic products 3, 8, and 14 showed a highly similar glutamate backbone NMR chemical shift and *J*-values despite the variable *N*-substituents, thereby supporting the relative β -position stereochemistry (Figure 4D; Tables S1, S2). Our cumulative kinetic and alternative substrate results suggest that the intramolecular cyclization reaction is fastest when substrate stereochemistry permits; however, intermolecular β -hydroxyl rebound occurs more quickly than 1,5-HAT and distal hydroxylation in saturated substrates. These results additionally confirm that the unique dual cyclization and hydroxylation activity observed with DabC are conserved across kainoid synthases from diverse biological species and biosynthetic pathways. Moreover, this approach exemplifies the use of non-native substrates to interrogate wild-type enzyme mechanisms.

The substrate-dependent chemoselectivity of kainoid synthases, although uncommon, has precedent within the Fe/ α KG enzyme family. L-Norvaline halogenase SyrB2 from *Pseudomonas syringae* is capable of hydroxylation on both L-threonine and L-aminobutyric acid.²³ Fungal L-valine/L-isoleucine aziridinase TqaL similarly shows stereoselective hydroxylation activity on a simplified substrate analogue.^{24,25} Substantial engineering efforts have improved the interconversion of select Fe/ α KG hydroxylases into halogenases, and broader application to other homologues and substrates is under active investigation.^{26–28} Given the utility of Fe/ α KGs to regio- and stereoselectively functionalize C–H bonds on chemically complex scaffolds, members of this enzyme family have seen extensive biocatalytic application. From the syntheses of bioactive *ent*-kaurane diterpenoid²⁹ and tropolone natural products,³⁰ the preparation of isotopically enriched standards for the quantifiable detection of cyanotoxin cylindrospermopsin³¹ or the scalable biotransformation of KA,¹² chemoenzymatic methods using Fe/ α KGs help circumvent synthetic challenges and improve overall efficiency in the production of natural products, pharmaceuticals, and small molecule tools. The dual functionality seen in the algal kainoid synthases showcases their flexible chemoselectivities on relatively conservative substrate analogues. Further investigation into these unique homologues will provide additional insight into the understanding, engineering, and application of the chemically useful and diverse Fe/ α KG family.

■ ASSOCIATED CONTENT

Supporting Information

The Supporting Information is available free of charge at <https://pubs.acs.org/doi/10.1021/acschembio.3c00596>.

General materials and methods, molecular biology and biochemical methods, enzyme assay methods, supplementary Figures and Tables, chemical synthesis, and NMR spectra (PDF)

■ AUTHOR INFORMATION

Corresponding Author

Shaun M. K. McKinnie – Department of Chemistry and Biochemistry, University of California, Santa Cruz, Santa Cruz, California 95064, United States; orcid.org/0000-0001-6776-6455; Email: smckinnie@ucsc.edu

Author

Austin R. Hopiavuori – Department of Chemistry and Biochemistry, University of California, Santa Cruz, Santa Cruz, California 95064, United States; orcid.org/0000-0002-7093-7558

Complete contact information is available at:

<https://pubs.acs.org/doi/10.1021/acschembio.3c00596>

Author Contributions

A.R.H. and S.M.K.M. designed this study. Small molecule organic synthesis, characterization, protein expression and purification, and enzyme assays and kinetics were performed by A.R.H. The manuscript was written through contributions of all authors, and all authors have given approval to the final version.

Notes

The authors declare no competing financial interest.

■ ACKNOWLEDGMENTS

This work was supported by the University of California, Santa Cruz (startup funding) and the National Institutes of Health (R21-GM148870-01). We gratefully acknowledge L. Sanchez and G. Luu for assistance obtaining high-resolution mass spectrometry data, H.-W. Lee for maintenance of nuclear magnetic resonance spectroscopy facilities, J. MacMillan for access to high-performance liquid chromatography (all University of California, Santa Cruz). The authors also thank J. Chekan (University of North Carolina at Greensboro) for helpful discussions.

■ REFERENCES

- (1) Hausinger, R. P. Fe(II)/ α -ketoglutarate-dependent hydroxylases and related enzymes. *Crit. Rev. Biochem. Mol. Biol.* **2004**, *39*, 21–68.
- (2) Gao, S.-S.; Naowarajna, N.; Cheng, R.; Liu, X.; Liu, P. Recent examples of α -ketoglutarate-dependent mononuclear non-haem iron enzymes in natural product biosyntheses. *Nat. Prod. Rep.* **2018**, *35*, 792–837.
- (3) Zwick, C. R.; Renata, H. Overview of amino acid modifications by iron- and α -ketoglutarate-dependent enzymes. *ACS Catal.* **2023**, *13*, 4853–4865.
- (4) Yin, X.; Zabriskie, T. M. VioC is a non-heme iron, α -ketoglutarate-dependent oxygenase that catalyzes the formation of 3*S*-hydroxy-L-arginine during viomycin biosynthesis. *ChemBioChem.* **2004**, *5*, 1274–1277.
- (5) Eichhorn, E.; van der Ploeg, J. R.; Kertesz, M. A.; Leisinger, T. Characterization of α -ketoglutarate-dependent taurine dioxygenase from *Escherichia coli*. *J. Biol. Chem.* **1997**, *272*, 23031–23036.

- (6) Obermaier, S.; Müller, M. Ibotenic acid biosynthesis in the fly agaric is initiated by glutamate hydroxylation. *Angew. Chem., Int. Ed.* **2020**, *59*, 12432–12435.
- (7) Tang, M.-C.; Zou, Y.; Watanabe, K.; Walsh, C. T.; Tang, Y. Oxidative cyclization in natural product biosynthesis. *Chem. Rev.* **2017**, *117*, 5226–5333.
- (8) Shimo, S.; Ushimaru, R.; Engelbrecht, A.; Harada, M.; Miyamoto, K.; Kulik, A.; Uchiyama, M.; Kaysser, L.; Abe, I. Stereodivergent nitrocyclopropane formation during biosynthesis of belactosins and hormaomycins. *J. Am. Chem. Soc.* **2021**, *143*, 18413–18418.
- (9) Lau, W.; Sattely, E. S. Six enzymes from mayapple that complete the biosynthetic pathway to the etoposide aglycone. *Science* **2015**, *349*, 1224–1228.
- (10) Chang, W.; Yang, Z.-J.; Tu, Y.-H.; Chien, T.-C. Reaction mechanism of a nonheme iron enzyme catalyzed oxidative cyclization via C-C bond formation. *Org. Lett.* **2019**, *21*, 228–232.
- (11) Brunson, J. K.; McKinnie, S. M. K.; Chekan, J. R.; McCrow, J. P.; Miles, Z. D.; Bertrand, E. M.; Bielinski, V. A.; Luhavaya, H.; Obornik, M.; Smith, G. J.; Hutchins, D. A.; Allen, A. E.; Moore, B. S. Biosynthesis of the neurotoxin domoic acid in a bloom-forming diatom. *Science* **2018**, *361*, 1356–1358.
- (12) Chekan, J. R.; McKinnie, S. M. K.; Moore, M. L.; Poplawski, S. G.; Michael, T. P.; Moore, B. S. Scalable biosynthesis of the seaweed neurochemical, kainic acid. *Angew. Chem., Int. Ed.* **2019**, *58*, 8454–8457.
- (13) Steele, T. S.; Brunson, J. K.; Maeno, Y.; Terada, R.; Allen, A. E.; Yotsu-Yamashita, M.; Chekan, J. R.; Moore, B. S. Domoic acid biosynthesis in the red alga *Chondria armata* suggests a complex evolutionary history for toxin production. *Proc. Natl. Acad. Sci. U. S. A.* **2022**, *119*, No. e2117407119.
- (14) Tian, Z.; Clark, B. L. M.; Menard, F. Kainic acid-based agonists of glutamate receptors: SAR analysis and guidelines for analog design. *ACS Chem. Neurosci.* **2019**, *10*, 4190–4198.
- (15) McCabe, R. M.; Hickey, B. M.; Kudela, R. M.; Lefebvre, K. A.; Adams, N. G.; Bill, B. D.; Gulland, F. M. D.; Thomson, R. E.; Cochlan, W. P.; Trainer, V. L. An unprecedented coastwide toxic algal bloom linked to anomalous ocean conditions. *Geophys. Res. Lett.* **2016**, *43*, 10366–10376.
- (16) Maeno, Y.; Kotaki, Y.; Terada, R.; Cho, Y.; Konoki, K.; Yotsu-Yamashita, M. Six domoic acid related compounds from the red alga, *Chondria armata*, and domoic acid biosynthesis by the diatom, *Pseudo-nitzschia multiseriata*. *Sci. Rep.* **2018**, *8*, 356.
- (17) da Silva, F. M.; da Silva, A. M. P. W.; Mittersteiner, M.; Andrade, V. P.; Aquino, E. da C.; Bonacorso, H. G.; Martins, M. A. P.; Zanatta, N. Regio- and stereoselective synthesis of polysubstituted 5-hydroxypyrrolidin-2-ones from 3-alkoxysuccinimides. *Tetrahedron Lett.* **2020**, *61*, 151358.
- (18) Oba, M.; Mita, A.; Kondo, Y.; Nishiyama, K. Facile synthesis of 3-hydroxyglutamic acids via cyanation of chiral *N*-acyliminium cation derived from (*S*)-malic acid. *Synth. Commun.* **2005**, *35*, 2961–2966.
- (19) Chen, T.-Y.; Xue, S.; Tsai, W.-C.; Chien, T.-C.; Guo, Y.; Chang, W. Deciphering pyrrolidine and olefin formation mechanism in kainic acid biosynthesis. *ACS Catal.* **2021**, *11*, 278–282.
- (20) Maeno, Y.; Kotaki, Y.; Terada, R.; Hidaka, M.; Cho, Y.; Konoki, K.; Yotsu-Yamashita, M. Preparation of domoic acid analogues using a bioconversion system, and their toxicity in mice. *Org. Biomol. Chem.* **2021**, *19*, 7894–7902.
- (21) Stateman, L. M.; Nakafuku, K. M.; Nagib, D. A. Remote C-H functionalization via selective hydrogen atom transfer. *Synthesis (Stuttg)* **2018**, *50*, 1569–1586.
- (22) Rui, J.; Zhao, Q.; Huls, A. J.; Soler, J.; Paris, J. C.; Chen, Z.; Reshetnikov, V.; Yang, Y.; Guo, Y.; Garcia-Borràs, M.; Huang, X. Directed evolution of nonheme iron enzymes to access abiological radical-relay C(sp³)-H azidation. *Science* **2022**, *376*, 869–874.
- (23) Matthews, M. L.; Neumann, C. S.; Miles, L. A.; Grove, T. L.; Booker, S. J.; Krebs, C.; Walsh, C. T.; Bollinger, J. M. Substrate positioning controls the partition between halogenation and hydroxylation in the aliphatic halogenase. *SyrB2. Proc. Natl. Acad. Sci. U. S. A.* **2009**, *106*, 17723–17728.
- (24) Cha, L.; Paris, J. C.; Zanella, B.; Spletzer, M.; Yao, A.; Guo, Y.; Chang, W. Mechanistic studies of aziridine formation catalyzed by mononuclear non-heme iron enzymes. *J. Am. Chem. Soc.* **2023**, *145*, 6240–6246.
- (25) Tao, H.; Ushimaru, R.; Awakawa, T.; Mori, T.; Uchiyama, M.; Abe, I. Stereoselectivity and substrate specificity of the Fe(II)/ α -ketoglutarate-dependent oxygenase TqaL. *J. Am. Chem. Soc.* **2022**, *144*, 21512–21520.
- (26) Papadopoulou, A.; Meierhofer, J.; Meyer, F.; Hayashi, T.; Schneider, S.; Sager, E.; Buller, R. Re-programming and optimization of a L-proline *cis*-4-hydroxylase for the *cis*-3-halogenation of its native substrate. *ChemCatChem* **2021**, *13*, 3914–3919.
- (27) Neugebauer, M. E.; Kissman, E. N.; Marchand, J. A.; Pelton, J. G.; Sambold, N. A.; Millar, D. C.; Chang, M. C. Y. Reaction pathway engineering converts a radical hydroxylase into a halogenase. *Nat. Chem. Biol.* **2022**, *18*, 171–179.
- (28) Kastner, D. W.; Nandy, A.; Mehmood, R.; Kulik, H. J. Mechanistic insights into substrate positioning that distinguish non-heme Fe(II)/ α -ketoglutarate-dependent halogenases and hydroxylases. *ACS Catal.* **2023**, *13*, 2489–2501.
- (29) Zhang, X.; King-Smith, E.; Dong, L.-B.; Yang, L.-C.; Rudolf, J. D.; Shen, B.; Renata, H. Divergent synthesis of complex diterpenes through a hybrid oxidative approach. *Science* **2020**, *369*, 799–806.
- (30) Perkins, J.; Gollhofer, A.; Hernández-Meléndez, J.; Saucedo, A.; Doyon, T.; Narayan, A. Enzyme library-enabled chemoenzymatic tropolone synthesis. *ChemRxiv*, June 13, 2023, ver. 1. DOI: 10.26434/chemrxiv-2023-lvngd.
- (31) Mailyan, A. K.; Chen, J. L.; Li, W.; Keller, A. A.; Sternisha, S. M.; Miller, B. G.; Zakarian, A. Short total synthesis of [¹⁵N₃]-cylindrospermopsins from ¹⁵NH₄Cl enables precise quantification of freshwater cyanobacterial contamination. *J. Am. Chem. Soc.* **2018**, *140*, 6027–6032.